Low Field Zeeman Magnetometry Using Rubidium Absorption Spectroscopy

Journal of Physics: Conference Series **80** (2007) 012035 doi:10.1088/1742-6596/80/1/012035

Low Field Zeeman Magnetometry Using Rubidium Absorption Spectroscopy

Nibedita Ram, M Pattabiraman[1], C Vijayan

Department of Physics, Indian Institute of Technology, Madras, Chennai 600036, India

Email: pattu@physics.iitm.ac.in

Abstract. We report on the feasibility of utilizing the field dependence of the Doppler-free unresolved absorption line amplitude of Rubidium vapour for magnetic field measurements for fields below 50 G. The field dependence of the saturation absorption and Doppler broadened fluorescence line amplitudes have been systematically analyzed by computing the hyperfine energy eigenvalues and the transition probability among the Zeeman sublevels.

1. Introduction

The Interaction of a laser beam with atoms in presence of magnetic field has been used for sensitive magnetometry in many different ways. These include magnetometers based on the Zeeman line shift [1], coherent population trapping, electromagnetically induced transparency [2, 3] the Hanle effect [4], and more recently nonlinear magneto-optic rotation [5, 6].Among these techniques, a precise measurement of the frequency shift between Zeeman transitions as a function of magnetic field in an absorbing medium allows the design of a magnetometer with moderate sensitivity. However, Zeeman splitting is usually well resolved only for fields above 50 Gauss and it is in this field region that such magnetometers based on the Zeeman effect operate.

We have studied the feasibility of utilizing the field dependence of the Doppler-free unresolved absorption line amplitude of Rubidium vapour for magnetic field measurements for fields below 50 G. The hyperfine energy eigenvalues and the transition probability of Zeeman sublevels have been computed between 0 -50 Gauss in an attempt to understand the observed field dependence of the line amplitude.

The total Hamiltonian **H** of an atom with total electronic angular momentum **J** and nuclear spin **I**, subject to magnetic field is [7]

$$H = A_{hfs}\mathbf{I}\cdot\mathbf{J} + B_{hfs}\frac{3(\mathbf{I}\cdot\mathbf{J})^2 + \frac{3}{2}\mathbf{I}\cdot\mathbf{J} - I(I+1)J(J+1)}{2I(2I-1)J(2J-1)} + \mu_B g_F \mathbf{F}\cdot\mathbf{B} \quad (1)$$

[1] To whom any correspondence should be addressed.

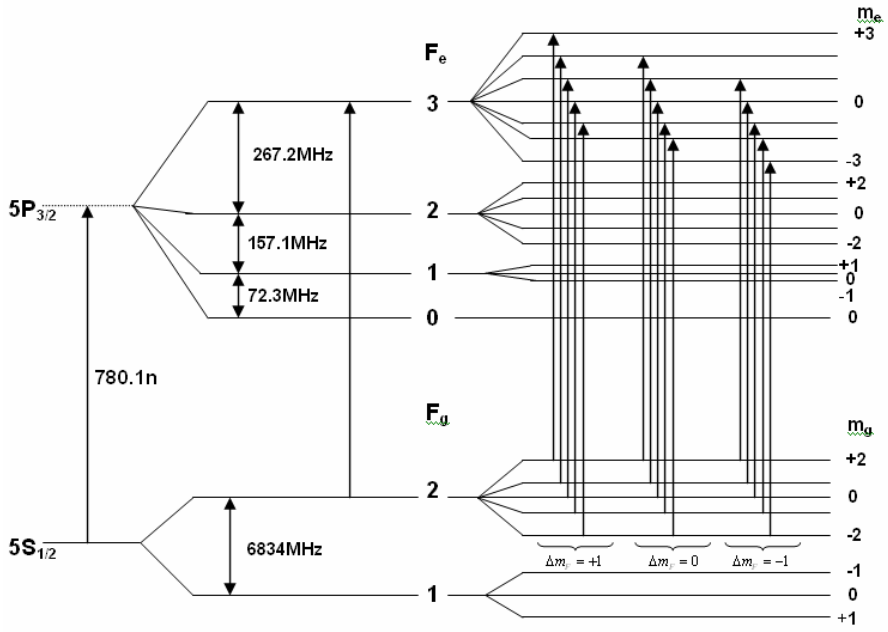

Figure 1: Energy level diagram for ^{87}Rb

Here the first two terms represent the hyperfine interaction with A_{hfs} the magnetic dipole constant and B_{hfs} the electric quadrupole constant (for J > ½). The last term is the Zeeman Hamiltonian appropriate for magnetic fields smaller than the hyperfine splitting.

Rubidium has a single electron outside the closed shell ([Kr] 5s1) and therefore has a simple energy level diagram making absorption spectroscopy convenient. Its ground state and first excited states are $5S_{1/2}$ and $5P_{1/2,3/2}$ respectively. The nuclear magnetic moment produces a hyperfine structure as shown in figure 1. The ground state of ^{87}Rb splits into two levels with F_g=1 & 2 and second excited state splits into four levels with F_e=0, 1, 2, 3 due to hyperfine interaction. In the presence of magnetic field each level with specific F value splits into 2F+1 Zeeman sublevels [8]. In the ground state with F=1, the Zeeman sublevels are inverted because the Lande g factor (g_F) for sublevels F=1 and F=2 are opposite in sign.

The high vapour pressure of Rubidium allows its use in a vapour cell at room temperature [9] and external cavity diode lasers of wavelength 780 nm and 795 nm can be conveniently used to access its excited states. The hyperfine absorption lines of Rb can be resolved by eliminating the effects of Doppler linewidth broadening using saturation spectroscopy. In the presence of a magnetic field the hyperfine levels split into Zeeman sublevels. The magnetic field couples the Zeeman sublevels corresponding to identical magnetic quantum numbers (m_F) but different total angular momentum quantum numbers, F, in the ground and excited states resulting in a nonlinear dependence of the energy eigenvalues with the magnetic field. As a result the magnetic quantum number F ceases to be a good quantum number since the magnetic sublevels of different F values mix. However m_F remains a good quantum number [10].

Among the two isotopes of rubidium, ^{87}Rb (I = 3/2; relative abundance 28 %) and ^{85}Rb (I= 5/2; relative abundance 72%), the latter exhibits significant Zeeman nonlinearity and crossings among the ground and excited state hyperfine levels even at magnetic fields (< 50 G) [10]. Therefore we chose ^{87}Rb to the study the field dependence of the absorption line amplitude

2. Experiment

The experimental set up for saturation/absorption spectroscopy is shown in figure 2. A Helmholtz coil is used to generate a uniform magnetic field in the region of the Rubidium vapour cell. For Rubidium

excitation we have used a commercial external cavity diode laser of 780nm. Saturation spectroscopy involves three beams (saturating, probe and reference) of light derived from the same laser that pass through a cell containing low density vapour of atoms (figure 2). The strong saturating beam depletes atoms in the initial state, leaving very few for the probe beam (passed in the opposite direction) to interact with, resulting in 'Lamb dips'. Only atoms which have no component of velocity in the direction of propagation of the beams absorb at the frequency associated with atoms at rest are at resonance with both beams. The velocity selective signal produced by the pump and the probe beams is subtracted from the signal obtained from a reference beam to produce Doppler-free spectral lines.

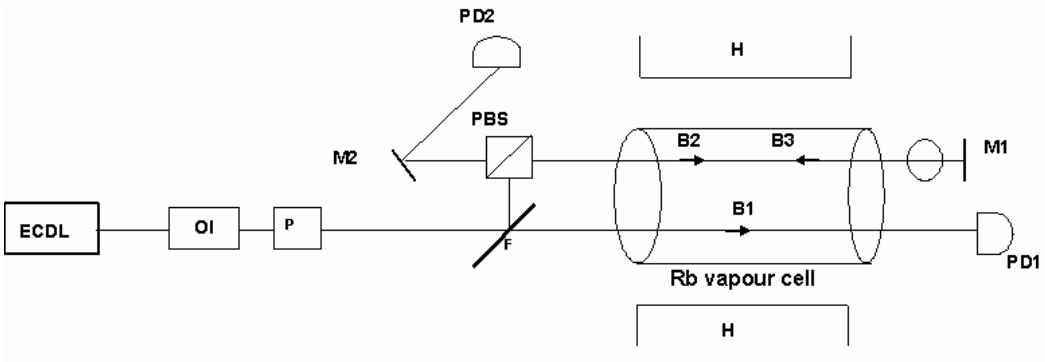

Figure 2: Schematic diagram of the experimental setup used. **Key: ECDL**-External Cavity Diode Laser, **OI**-Optical Isolator, **F**-Filter, **PD** -Photodiode, **M**-Mirror, **PBS**-Polarizing Beam Splitter, **H**-Helmholz coil, **B1**-Refference beam, **B2**-Pump beam, **B3**-Probe beam.

3. Results

The zero-field Doppler-broadened laser-induced fluorescence spectrum of Rb is shown in figure 3a. The laser-induced fluorescence profile on the D2 line consists of four peaks corresponding to two ground-state hyperfine components and an unresolved hyperfine structure for each of the two stable rubidium isotopes. The zero-field Doppler free saturation absorption spectrum for ^{87}Rb (F_g =2) is shown in figure 3b. The peaks observed in addition to the primary hyperfine resonances are called crossover resonances. They correspond to the pump and probe beam interacting with a certain velocity group via two different hyperfine transitions with a common lower level and occur when the laser is tuned halfway between two primary resonances.

The field dependence of the amplitude of the saturation absorption line F_g = 2 to F_e = 3 and crossover line F_g = 2 to F_e = 2 & 3 are shown in figure 4a and figure 4b. Up to nearly 50 G the Zeeman components remain unresolved and the amplitude of the envelope was measured. The amplitude peaks around 10 G in both plots as observed earlier [11]. Above and below 10 G both spectral amplitudes decrease reproducibly in a near linear fashion. It is this feature that we suggest could be exploited for magnetic field measurements. The decrease in signal amplitude can be reliably correlated to the applied magnetic field by locking the wavelength of the external cavity diode laser to the top of the absorption of interest. Measurements with higher signal to noise could be performed by modulating the laser excitation current and by using lock-in detection to measure the signal amplitude. Such improvements are currently underway.

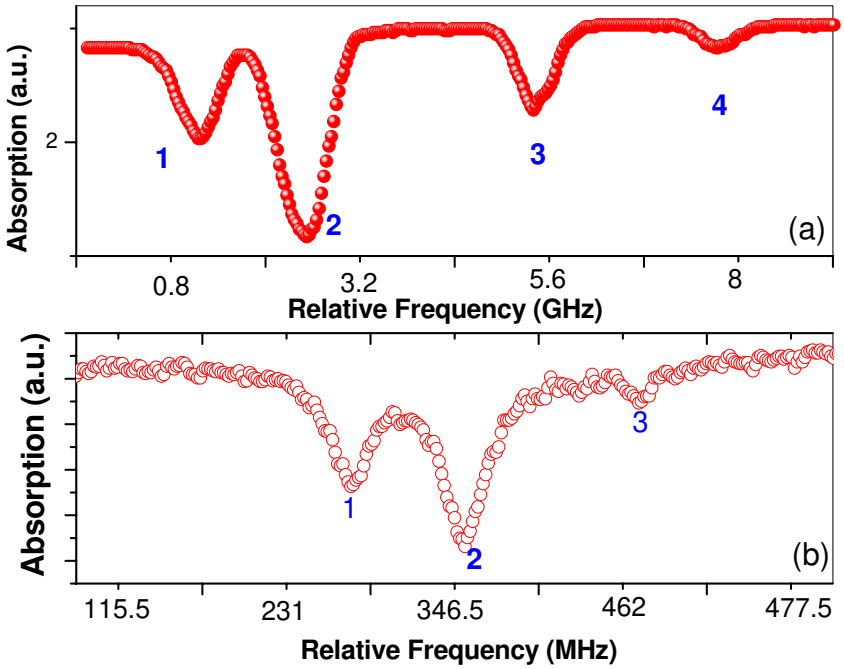

Figure 3. (a) Absorption spectrum for 87Rb and 85Rb. '1' denotes transition between Fg=2 to Fe=1,2,3 for 87Rb; '2': transition between Fg =3 to Fe=2,3,4 for 85Rb; '3': transition between Fg=2 to Fe=1,2,3 for 85Rb; '4': transition between Fg=1 to Fe=0,1,2 for 87Rb**. (b)** Saturation signal for 87Rb (Fg=2 to Fe=1, 2, 3). '1' denotes crossover transition of Fg=2 to Fe=2&3; '2': crossover transition of Fg=2 to Fe=1&3; '3': hyperfine transition of Fg=2 to Fe=3.

Since the setup can in principle be rendered portable this technique could be used to detect cracks in pipelines and structures using magnetic steel which usually have a remnant magnetization of a few Gauss. Any crack would result in an enhanced field value which could be detected as a decrease in signal amplitude. Since the peak around 10 G is reproducibly observed it might be used as a field marker for bar magnet inspection and a pressure marker in diamond anvil cells.

4. Discussion

We now consider the origin of the peak in intensity around 10 G. Saturation spectra exhibit several peculiarities such as inverted crossover peaks [12, 13] and are related to optical pumping effects in the presence of a magnetic field. In order to determine whether the 10 G amplitude peak is related to saturation spectroscopy we measure the field dependence of the amplitude of the corresponding fluorescence spectrum (by blocking beams B2 and B3 in figure 2) for $F_g = 2$ to $F_e = 1,2,3$ (figure 5a). We found a similar peak around 10 G and it was found to be reasonably reproducible (figure 5b).

Thus it is clear that the 10 G amplitude peak arises from simple fluorescence. A comparison of figures 5a and (4a, 4b) shows that using saturation spectra results in a nearly linear behaviour below 10 G unlike the fluorescence amplitude. Thus in addition to better spectral resolution and higher signal to noise ratio, it may be possible to extend saturation spectral amplitude based magnetometry to low fields by using a magnetic shield around the Rb cell.

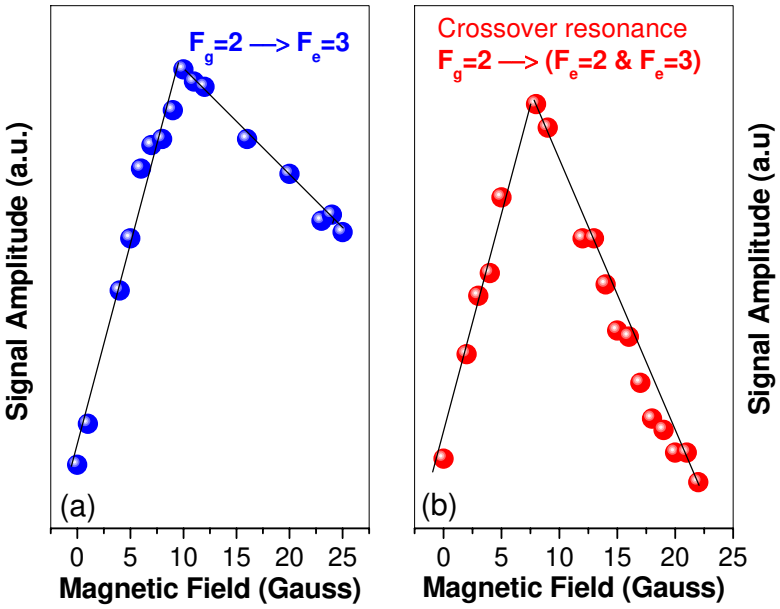

Figure 4: (a) Plot of signal amplitude versus magnetic field for the F_g=2 to F_e=3 transition. **(b)** Plot of signal amplitude versus magnetic field for the crossover line of Fg=2 to Fe= 2 & 3.

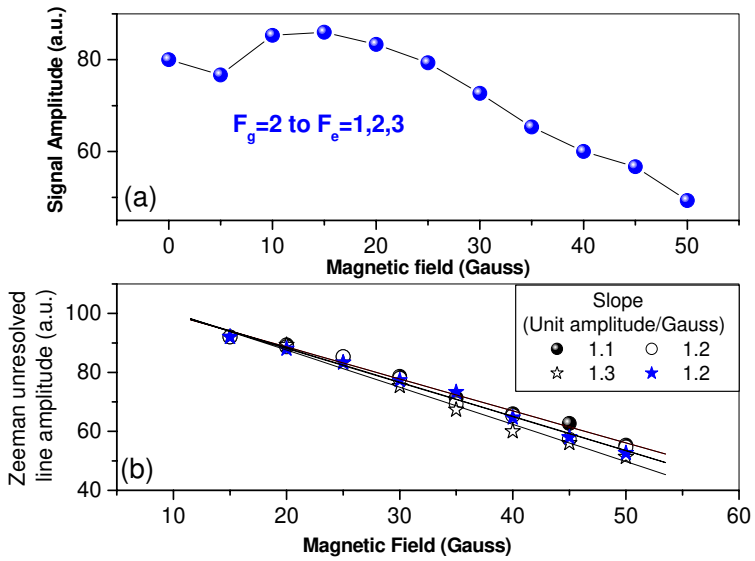

Figure 5: (a) Plot of signal amplitude versus magnetic field for unresolved Zeeman line from Fg=2 to Fe=1, 2, 3. **(b)** Plot of signal amplitude versus magnetic field for unresolved Zeeman line from Fg=2 to Fe=1, 2, 3 above 10 gauss which is reproducibly linear.

Previous studies concerning line intensities by Bowie et. al. [14] report a significant influence of magnetic fields of the order of 10 mT. Surprisingly we were unable to find a report that describes the field dependence of the signal intensity/amplitude for fields < 50 G in Rubidium. Therefore to understand the origin of this peak we consider the two closely related effects of turning on a magnetic field: (a) nonlinear dependence of the hyperfine energy levels and (b) mixing of the magnetic sublevels.

The energy levels correspond to the eigenvalues obtained by diagonalizing the Hamiltonian in equation 1. The eigenvalues thus obtained for the ground state ($5S_{1/2}$) and second excited state ($5P_{3/2}$) for ^{87}Rb are shown in figure (6a, 6b). The electric quadruple term, B_{hfs}, is neglected in this computation. We consider the transition $F_g=2 \rightarrow F_e = 3$ corresponding to the data presented in figure 4. From figure 6 it is clear that below 50 G, all excited and ground state hyperfine levels are nearly linear and that there are no level crossings, barring F = 1. Therefore nonlinear Zeeman splitting and/or level crossings are unlikely to cause the 10 G amplitude peak for $F_g=2 \rightarrow F_e = 3$.

In order to study the effect of hyperfine magnetic sublevel mixing on the line intensities it is necessary to compute the transition probabilities of each Zeeman sublevel as described below.

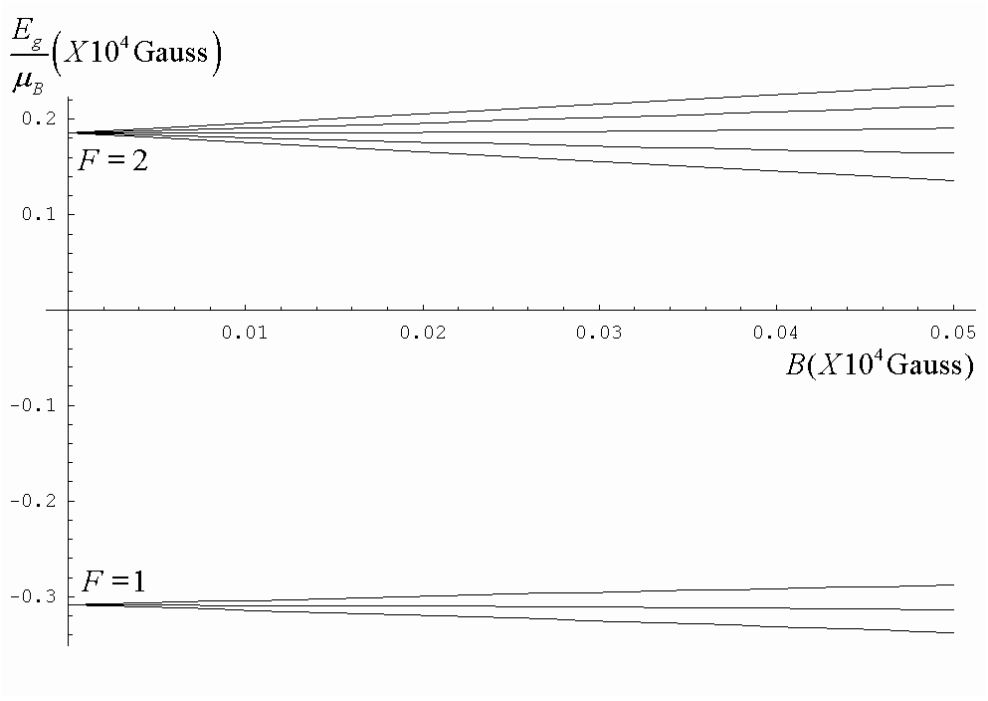

Figure 6: (a) Magnetic field dependence of ^{87}Rb ground state ($5S_{1/2}$) hyperfine energy levels.

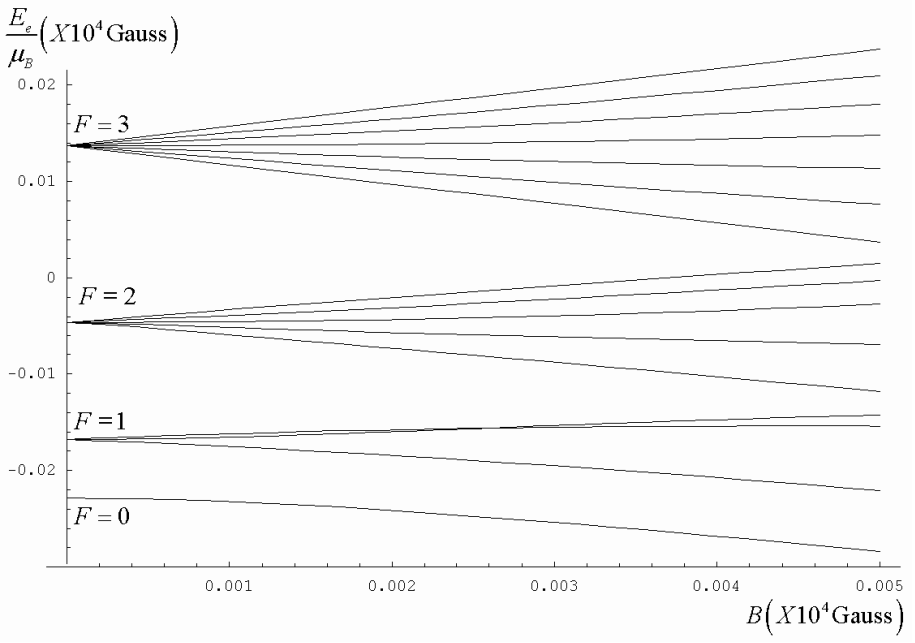

Figure 6: (b) Magnetic field dependence of ^{87}Rb excited state ($5P_{3/2}$) hyperfine energy levels.

4.1 Computation of Transition Probabilities

The mixed states can be represented by a superposition of the base kets for the ground and excited states [15]

$$\left|\psi(F_g,m_g)\right\rangle=\sum_g C_{gg'}\left(B,m_g\right)\left|F_{g'},m_g\right\rangle \text{ Ground states} \quad (2)$$

$$\left|\psi\left(F_e,m_e\right)\right\rangle=\sum_{e'} C_{ee'}\left(B,m_e\right)\left|F_{e'},m_e\right\rangle \text{ Excited states} \quad (3)$$

Where the summation is performed only on eigenvectors with same m_F (= m_g or m_e) values since the perturbation introduced by applied magnetic field couples only states with same m_F values. The mixing coefficients $C_{gg'}\left(B,m_g\right)$ and $C_{ee'}\left(B,m_e\right)$ depend on the magnetic field. For simplicity in the rest of the paper we shall denote the unmixed total angular momentum quantum number as $F_e'\left(F_g'\right)$ and the new quantum number as $F_e\left(F_g\right)$.

Upon application of a laser field the probability of transition among the between the ground and excited state hyperfine sublevels is given by the Fermi's Golden Rule,

$$W_{eg}=\frac{\left|\left\langle\psi(F_e,m_e)\right|\mathbf{D}.\mathbf{e}\left|\psi(F_g,m_g)\right\rangle\right|^2 E^2}{4\hbar^2}\delta(v-v_{eg}-V.k/2\pi) \quad (4)$$

Where **E, e** and ν are the electric field amplitude, unit vector and the laser frequency respectively. The transition frequency is given by $v_{eg}=\left[\left(E_e-E_g\right)/h\right]$. V is atomic velocity and k is propagation vector. The electric dipole moment can be written as $\mathbf{D}.\mathbf{e}=\sum_q D_q e_q$, where q=-1, 0, +1. The matrix

element of a given dipole component D_q is proportional to the spontaneous emission rate of the associated transition A_{eg},

$$\left|\left\langle\psi(F_e,m_e)\right|D_q\left|\psi(F_g,m_g)\right\rangle\right|^2=\frac{3\varepsilon_0\hbar\lambda_{eg}^3}{8\pi^2}A_{eg} \quad (5)$$

The spontaneous emission rate is proportional to the square of the transfer coefficient modified by the presence of magnetic field,

$$A_{eg}=\Gamma_e a^2\left[\psi\left(F,m_e\right);\psi\left(F_g,m_g\right);q\right] \quad (6)$$

These modified transfer coefficients are expressed as

$$a\left[\psi\left(F_e,m_e\right);\psi\left(F_g,m_g\right)\right]=\sum_{F_e^{'}F_e^{'}}C_{F_eF_e^{'}}a\left(F_e^{'},m_e;F_g^{'},m_g;q\right)C_{F_gF_g^{'}} \quad (7)$$

Where

$$a\left(F_e,m_e;F_g,m_g;q\right)=(-1)^{1+I+J_e+F_e+F_g-m_e}\sqrt{2J_e+1}\sqrt{2F_e+1}\sqrt{2F_g+1}\times \begin{pmatrix} F_e & 1 & F_g \\ -m_e & q & m_g \end{pmatrix}\begin{Bmatrix} F_e & 1 & F_g \\ J_e & I & J_e \end{Bmatrix} \quad (8)$$

are the unperturbed transfer coefficients. The parentheses and curly brackets denote the 3-j and 6-j coefficients respectively. Thus field dependence of the transition probabilities among Zeeman sublevels originates from the field dependence of the mixing coefficients $C_{gg^{'}}\left(B,m_g\right)$ and $C_{ee^{'}}\left(B,m_e\right)$. These are obtained as eigenvectors by diagonalizing the Hamiltonian in equation 1.

We compute the square of the modified transfer coefficients, $a^2\left[\psi\left(F,m_e\right);\psi\left(F_g,m_g\right);q\right]$ (which are proportional to the field induced change in the transition probability) for transitions among the Zeeman sublevels $F_g=2\rightarrow F_e=3$ [16]. The computed transfer coefficients for the 15 transitions possible (5 each corresponding to the selection rule $\Delta m_F = 0, +1, -1$) are shown in figure 7.

All modified transfer coefficients either increase or decrease monotonically up to 50 G. Therefore the sum of the modified transfer coefficients which is proportional to the transition probability of the unresolved Zeeman line considered in this study, is featureless around 10 G. A similar result is inferred from a previous study by Tremblay et al. who considered the $F_g=2\rightarrow F_e=2$ transition in ^{87}Rb [17]. Thus the 10 G amplitude peak for $F_g=2\rightarrow F_e=3$ and the crossover $F_g = 2\rightarrow F_e= 2$ & 3 peak cannot be explained by the nonlinear energy eigenvalues and the mixing of the magnetic sublevel of the hyperfine levels. Could this occur due to a preferential mixing of hyperfine levels? Is the $(5P_{3/2})F=1$ state which exhibits significant low field nonlinearity involved in such a mixing although it is not involved in the transitions under study? In order to address such outstanding questions, further experiments (involving other hyperfine levels with different light polarizations) and perhaps a modified representation of $\left|\psi(F_g,m_g)\right\rangle$ and $\left|\psi(F_e,m_e)\right\rangle$ may be necessary to account for the 10 G amplitude peak.

In conclusion the field dependence of the saturation absorption and Doppler broadened fluorescence line amplitudes have been systematically analyzed by computing the hyperfine energy eigenvalues and the transition probability among the Zeeman sublevels. The magnetic field dependence of the absorption and saturation line amplitudes exhibits a peak around 10 G. The linear field dependent intensity on either side of the 10 G peak maybe exploited for magnetic field measurements. The origin of the 10 G peak however could not be explained on the basis of the computed field dependence of the transition probability among hyperfine Zeeman sublevels and further studies are needed in this direction.

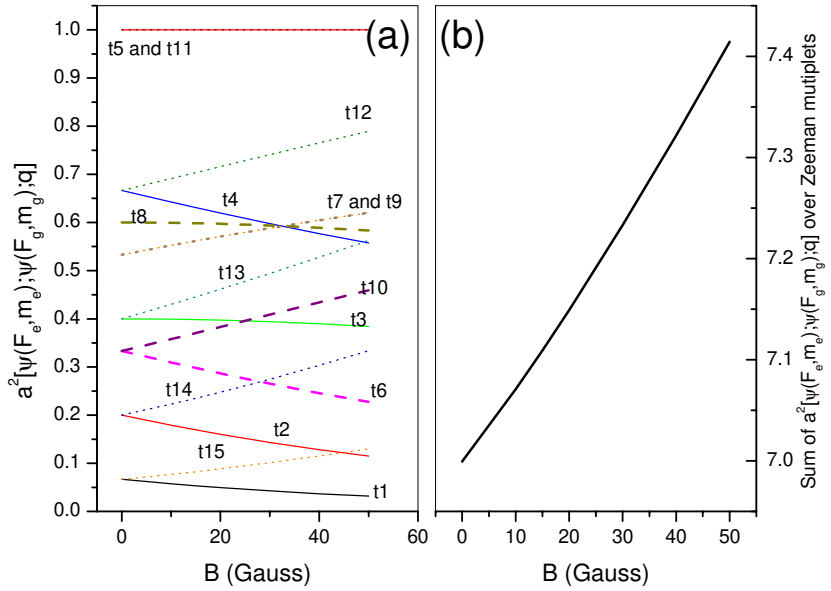

Figure 7: (a) Plot of the square of transfer coefficient versus magnetic field for all the fifteen possible transitions between F_g=2 to F_e=3. **Key:** t_1→ F_g=2, m_g =+2 to F_e=3, m_e=+1; t_2→F_g=2, m_g =+1 to F_e=3, m_e=0; t_3→F_g=2, m_g =0 to F_e=3, m_e=-1; t_4→F_g=2, m_g =-1to F_e=3, m_e=-2; t_5→F_g=2, m_g =-2 to F_e=3, m_e=-3; t_6→F_g=2, m_g =+2 to F_e=3, m_e=+2; t_7→F_g=2, m_g =+1 to F_e=3, m_e=+1; t_8→F_g=2, m_g =0 to F_e=3, m_e=0; t_9→F_g=2, m_g =-1 to F_e=3, m_e=-1; t_{10}→F_g=2, m_g =-2 to F_e=3, m_e=-2; t_{11}→F_g=2, m_g =+2 to F_e=3, m_e=+3; t_{12}→F_g=2, m_g =+1 to F_e=3, m_e=+2; t_{13}→F_g=2, m_g =0 to F_e=3, m_e=+1; t_{14}→F_g=2, m_g =-1 to F_e=3, m_e=0; t_{15}→F_g=2, m_g =-2 to F_e=3, m_e=-1.

(b) Plot for sum of square of transfer coefficients versus magnetic field for the fifteen transitions between Fg=2 to Fe=3.

References

[1] Sarkisyan D G, Popayan A V, Varzhapetyan T S, Blush K, Auzinsh M, *J. Optics and Spectroscopy,***96**,328 (2004)
[2] Affolderbach C, Stahler M, Knappe S, Wynands R, J. *Appl. Phys. B* **75**605 (2002)
[3] Wynands R and Nagel A*, J. Appl. Phys. B,***68,** 1 (1999)
[4] Alnis J, Blushs K, Auznish M, Kennedy S, Ray N S and Abraham E R I, *J. Phys.B:At. Mol. Opt. Phys.***36,** 1173 (2003)
[5] Budker D, Kimball D F, Rochester S M, Yashchuk V V and Zolotorev M, *Phys. Rev. A*, **62**, 043403 (2000)
[6] Budker D, Yashchuk V Vand Zolotorev M, *Phys.Rev.Lett* **81***,* 5788 (1998)
[7] Steck Daniel A., Rubidium ^{87}D line Data(2003). Available online at *george.ph.utexas.edu/~dsteck/alkalidata/rubidium87numbers.pdf*
[8] Lees Ho Seong , Park Sang Eon , Park Jong Dae and Cho Hyuck, *J. Opt. Soc. Am. B*, **11,** 558 (1993)
[9] Preston Daryl W, *Am. J. Phys* **64,**1432 (1996)
[10] Alnis J and Auzinsh M, *Phy. Rev. A,* **63,** 023407 (2001)
[11] Ummal Momeen M, Rangarajan G and Deshmukh P C, presented at the 20th International Conference on Atomic Physics, ICAP 2006, July 16-21, Innsbruck, Austria.
[12] Budker D ,Orlando D J and Yashchuk V V, *Am. J. Phys.* **67**, 584 (1999)
[13] Kim S, Park S E, Lee H S, Oh C H, Park J D, and Cho H, *Jpn. J. Appl. Phys.,* Part 1, **32**, 3291 (1993)
[14] Bowie Jason, Boyle Jack and Chiao Raymond , *J. Opt. Soc. Am.B,***12,** 2946 (1995)
[15] Tremblay P, Michaud A, Levesque M, Theriault S, Breton M, Beaubien J and Cyr N, *Phy. Rev. A* **42**, 2766 (1990)
[16] Computed with a mathematica code available at *www.physics.umd.edu/courses/phys721/* (W D Phillips, Department of Physics, University of Maryland)
[17] Tremblay P, Michaud A,Beaubien A, Levesque A, Theriault S, Breton M, Cyr N,. Tetu M and Villeneuve B, Precision Electromagnetic Measurements, 1990. CPEM '90 Digest., Conference Iss., 11-14, 426 (1990). Available at *http://ieeexplore.ieee.org/xpls/abs_all.jsp?arnumber=110089*